Published in final edited form as:
Sci Signal. ; 2(102): ra86. doi:10.1126/scisignal.2000217.

CBL CONTROLS EGF RECEPTOR FATE BY REGULATING EARLY ENDOSOME FUSION[#]

Gina D. Visser Smit[1,3,‡], **Trenton L. Place**[1,‡], **Sara L. Cole**[2,3,‡], **Kathryn A. Clausen**[1,3], **Soumya Vemuganti**[1,3], **Guojuan Zhang**[2], **John G. Koland**[1], and **Nancy L. Lill**[2,3,*]

[1]Department of Pharmacology, University of Iowa, Iowa City, IA 52242

[2]Department of Pathology and the OSU Comprehensive Cancer Center, The Ohio State University, Columbus, OH 43210

Abstract

Residues 1-434 of the ubiquitin ligase Cbl control epidermal growth factor receptor (EGF-R) signaling by enhancing receptor ubiquitination, downregulation, and lysosomal degradation. Cbl 1-434 comprises a tyrosine kinase-binding domain, linker region, RING finger (RF), and a subset of the RF tail amino acids 420-436. Using full-length alanine substitution mutants, we demonstrate that the Cbl RF tail regulates biochemically distinct EGF-R endocytosis checkpoints: 1) Cbl- and ubiquitin-dependent degradation of hSprouty2 upstream of EGF-R ubiquitination (compromised by Cbl V431A); and 2) Cbl- and EGF-R-dependent dephosphorylation or degradation of the endosomal trafficking regulator Hrs (compromised by Cbl F434A). Deregulated Hrs phosphorylation correlates with the inhibition of both early endosome fusion and EGF-R degradation. This is the first evidence that Cbl can regulate receptor fate by controlling the fusion of sorting endosomes. We postulate that it does so by modulating the generation and loss of tyrosine phosphorylated Hrs.

Introduction

The ubiquitin ligase Cbl suppresses signaling from numerous receptor tyrosine kinases, including the epidermal growth factor receptor (EGF-R). Signal suppression is due, at least in part, to terminal routing of the kinases to lysosomes where they are degraded. Cbl controls EGF-R degradation at a post-internalization trafficking checkpoint that remains ill-defined [1-4]. It is widely accepted that Cbl-mediated receptor monoubiquitination or polyubiquitination is critical for the downregulation and lysosomal degradation of activated EGF-R [5-8]. However, receptor fate also is influenced by the posttranslational modification of other Cbl-associated proteins at the cell surface and on endosomes [4,9,10].

Several of these modifications require the presence of Cbl RING finger tail amino acids 420-434 [4]. This region was structured in a solved co-crystal of Cbl residues 47-434 and the E2/ubiquitin-conjugating enzyme UbcH7 [11]. RF tail stability was attributed, at least in part, to crystal packing. Several RF tail amino acids (I429; V430; D432; P433) appeared to participate in intramolecular interactions that might affect Cbl folding and function. Other

‡These authors contributed equally to the work.
[3]Some results reported here were generated while these authors were affiliated with the University of Iowa.
*To whom correspondence should be addressed: The Ohio State University, Department of Pathology, 139 Hamilton Hall, 1645 Neil Avenue, Columbus, OH 43210. Tel.: 614-247-8051; Fax: 614-293-2779; nancy.lill@osumc.edu

residues, including V431 and F434, played no obvious role in intramolecular or intermolecular interactions. Importantly, the structural results did not demonstrate a functional role for any RF tail residue in EGF-R regulation by Cbl.

We hypothesized that the Cbl RF tail controls EGF-R endocytosis and degradation at a trafficking checkpoint downstream of receptor internalization. To test this hypothesis, we utilized full-length RF tail substitution mutants. The strategic benefit of expressing dominant Cbl mutants is their ability to override the redundant regulation of EGF-R by all three endogenous Cbl proteins (c-Cbl, Cbl-b, and Cbl-3) without requiring their simultaneous knock-down. Through our analysis of RF tail substitution mutants, we demonstrate for the first time that Cbl enhances EGF-R degradation by regulating the fusion of sorting endosomes.

Results

To investigate how the RF tail might control EGF-R fate, we performed alanine scanning mutagenesis of Cbl residues 428-436 (Fig. 1A). The resulting panel of full-length, green fluorescent protein (GFP)-tagged, single amino acid substitution mutants was tested for activity in assays of EGF-R downregulation (receptor loss from the cell surface), ubiquitination, and degradation (Fig. 1B-D, respectively). Most RF tail mutants functioned like wild type Cbl. Relative to the other mutants, Cbl P428A greater enhanced EGF-R downregulation and ubiquitination, but this did not translate to enhanced EGF-R degradation (Supporting Online Material - Fig. S1B). The V430A mutant induced significantly less receptor ubiquitination than did wild type Cbl, yet it retained the ability to enhance EGF-R downregulation and degradation. The V431A and F434A mutants were functionally compromised in all three assays. Because results from the V430A mutant established that a statistically significant decrease in receptor ubiquitination is not sufficient to compromise downregulation and degradation, this mutant was of minimal interest for further analysis. Instead, we focused on the fully defective mutants V431A and F434A.

We assessed the ability of the mutant proteins to bind to and enhance the degradation of the upstream Cbl target hSprouty2. Using HEK (human embryonic kidney) 293 cells, others have shown that hSprouty2 associates with Cbl's RING finger domain under conditions of ligand depletion, then binds to the Cbl TKB domain following receptor activation by ligand [12,13]. hSprouty2 translocation frees the RF for binding to an E2/ubiquitin-conjugating enzyme, a process required for Cbl-mediated ubiquitination [14]. Subsequent ubiquitination and degradation of TKB domain-associated hSprouty2 then facilitate TKB domain binding to activated EGF-R, leading to EGF-R ubiquitination [14-16]. Because Cbl V431A and F434A were defective for EGF-R ubiquitination, we asked whether either mutant was compromised for hSprouty2 binding or degradation. As in previous investigations of Sprouty2 degradation (4,12-16), an ectopically expressed epitope-tagged Sprouty2 protein was examined. This was done to compensate for the lack of commercially available antibodies effectively detecting endogenous Sprouty2. It also allowed us to track the fate of the Sprouty2 protein in transfected cells only, where the impact of ectopically expressed wild type and mutant GFP-Cbl proteins should be scored.

As shown in Figure 2A, all unstimulated cultures expressed similar levels of the GFP-Cbl proteins and FLAG epitope-tagged hSprouty2 (top and bottom panels, lanes 1, 5, 9, 13 and 17). hSprouty2 associated constitutively with the Cbl fusion proteins, as demonstrated by its recovery in anti-GFP immunoprecipitates [Fig. 2A, anti-GFP immunoprecipitation (I.P.) / FLAG immunoblot (I.B.) panel, 0-minute time points]. EGF treatment of the cells enhanced Cbl/Sprouty2 interactions. This was most apparent where the induced interactions were detected in the absence of Sprouty2 degradation (Fig. 2A, center FLAG panels, lanes 17 versus 18).

Most of the hSprouty2 protein appeared as a lower molecular mass doublet of approximately 42 kDa (Fig. 2A, species I and II), which has been shown by others to comprise nonphosphorylated and phosphorylated species. A FLAG-reactive band of approximately 50 kDa (species III) was detected only after cell stimulation with EGF. The apparent mass of the latter protein, its reactivity with anti-FLAG antibody, and its disappearance over the experimental time course suggested that it was monoubiquitinated hSprouty2.

When cells expressing wild type Cbl or the biochemically wild type mutants P433A and D432A were stimulated over a 20-minute period with EGF, Cbl/hSprouty2 complexes were progressively lost (Fig. 2A, anti-GFP I.P. / FLAG I.B. panels) and the total cellular pool of hSprouty2 was reduced (bottom panel). This depletion correlated with the appearance of ubiquitinated protein smears in anti-GFP immunoprecipitates [ubiquitin (Ub) I.B. panel, lanes 2-4, 10-12, and 14-16]. The protein smears likely comprise Cbl and Cbl-associated proteins bearing a variety of posttranslational modifications. The wild type activity of mutants D432A and P433A in this assay demonstrated that the integrity of the RF tail's consensus α-adaptin binding site [17], $_{432}$DPF$_{434}$, is not crucial for Cbl-mediated hSprouty2 degradation.

Expression of the RF tail mutant F434A reduced levels of Cbl-associated ubiquitinated proteins and induced hSprouty2 degradation to an extent similar to wild type Cbl (Fig. 2A Ub I.B. and bottom panels, respectively, compare lanes 5-8 to 1-4; Fig. S2A). Expression of the mutant V431A induced a severe defect in the ubiquitination of Cbl-associated proteins (Ub I.B. panel, lanes 17-20) and in hSprouty2 degradation: Cbl/hSprouty2 complexes persisted throughout the experimental stimulation period (FLAG I.B. panel, lanes 17-20), and there was no apparent decrease in the total cellular hSprouty2 pool (bottom panel, lanes 17-20). Both Cbl mutants retained the ability to associate with activated EGF-R (Fig. 1D). Thus, mutant V431A bound to both hSprouty2 and EGF-R and failed to mediate efficient ubiquitin-dependent degradation of either substrate, with a complete defect upstream in the EGF-R trafficking pathway at the site of Sprouty2 degradation. Mutant F434A was defective later in the pathway, as it effected significant Sprouty2 degradation but reduced EGF-R ubiquitination. These results argue that residues in close proximity within the RING finger tail differentially control the ubiquitination and degradation of distinct Cbl substrates.

We wished to determine whether different E2-binding abilities of the wild type and mutant Cbl proteins might explain their distinct activities, but in repeated experiments, we were unable to detect the association of any Cbl protein with endogenous UbcH7 (data not shown). It remains possible that another endogenous E2, such as Ubc5, binds differently to the wild type and mutant proteins.

We recently reported that ectopic expression of wild type Cbl enhances epidermal growth factor degradation, at least in part, by regulating phosphorylated hepatocyte growth factor-regulated tyrosine kinase substrate (Hrs) [9]. Hrs is an endosomal, 110 kDa EGF-R trafficking regulator that is inducibly phosphorylated on tyrosines 329 and 334 following cell stimulation with EGF [18,19]. Others had correlated Hrs tyrosine phosphorylation with the degradation of activated receptor tyrosine kinases [20-23]. We showed that Hrs phosphorylation is essential for efficient Cbl-mediated EGF-R degradation. We further showed that, in cells overexpressing wild type Cbl, the phosphoHrs signal is greatly enhanced and then rapidly depleted; this depletion corresponds to the degradation of phosphoHrs [9]. We therefore asked whether the RF tail mutant F434A, only mildly compromised for the ubiquitination and degradation of hSprouty2, was defective at the Hrs checkpoint downstream in the EGF-R trafficking pathway.

To compare the impacts of wild type Cbl and Cbl F434A on Hrs, lysate proteins from transfected HEK 293 cells were immunoblotted using a polyclonal antibody recognizing phosphorylated Hrs tyrosine 334 (pY334Hrs). Y334 is the principal Hrs site inducibly

phosphorylated downstream of EGF-activated EGF-R [18,19]. As shown in Figure 2B, expression of GFP-Cbl wt enhanced the EGF-induced pY334Hrs signal relative to the level observed for the GFP null control (top panel, compare lanes 9-12 to 1-4; Fig. S2B). In repeated studies of cells expressing GFP-Cbl wt, the pY334Hrs signal peaked at 5-10 minutes after the addition of ligand and decreased to near-baseline levels by 40 minutes post-stimulation. The E3-deficient Cbl mutants Y371F and V431A, which suppressed EGF-R downregulation and degradation (Figs. 1B, 1D), also suppressed Hrs pY334 phosphorylation (Fig. 2B top panel, compare lanes 5-8 and 17-20 to 1-4; Fig. S2B). These results were consistent with the proposed functional defect of the mutants upstream of Hrs, at the level of hSprouty2 regulation.

Cbl F434A and Cbl wt enhanced the pY334Hrs signal to similar levels after 10 minutes of cell stimulation (Fig. 2B top panel, compare lanes 11 and 15), but the F434A mutant was compromised for apparent pY334Hrs dephosphorylation/degradation at the 40-minute stimulation time point (compare lanes 12 and 16; Fig. S2B). This defect correlated with decreased EGF-R degradation, which is evaluated at the 90 minute stimulation time point (Fig. 1D). We conclude that Hrs tyrosine phosphorylation and timely Hrs dephosphorylation and/or destruction are critical determinants to target activated EGF receptors for degradation, and that both are regulated by the Cbl RF tail.

For the Hrs experiments, protein extracts were derived from cell pools containing both untransfected cells and cells transfected to express the GFP-tagged proteins of interest. The transfection efficiency ranged from 10-30% among experiments. Thus, the immunoblot signal for total Hrs in Fig. 2B reflects contributions from both transfected and untransfected cells. Because of this, the data cannot be used to compare: 1) the relative level of Cbl-mediated Hrs degradation; or 2) the ratio of phospho Hrs to total Hrs specifically in the cells ectopically expressing wild type versus F434A Cbl.

We next determined whether an EGF-R trafficking defect was apparent at the microscopic level in cells expressing GFP-Cbl F434A. Fixed cell immunofluorescence revealed that EGF-stimulated COS-7 cells expressing endogenous EGF-R with either wt GFP-Cbl or the F434A mutant contained enlarged, EEA1/EGF-R/GFP-positive early endosomes (Fig. 3). However, greater than 70% of the cells expressing Cbl mutant F434A exhibited endosome clustering and/or pairing.

To determine whether this phenotype reflected the delayed fusion of docked early endosomes, we performed live cell imaging of GFP-Cbl-expressing, EGF-stimulated COS-7 cells. Vesicle docking events were observed throughout the 40 minute imaging period. Some were evident in the first 30 seconds of image collection; others were initiated much later in the collection period. For consistency, fusion times were calculated as the minutes from docking to fusion for individual vesicle pairs, regardless of the stimulation time point at which their docking was initiated. Our results revealed that the fusion of docked early endosomes was rapid in cells expressing wild type Cbl, with most paired vesicles fusing within 30 seconds of docking (Fig. 4 A-B; Fig. S3). In cells expressing Cbl F434A, many paired endosomes failed to fuse, even after docking for 10 minutes or more (Fig. 4C; Fig. S4).

Expression of Cbl V431A typically resulted in a failure to generate even moderate-sized fused vesicles. Instead, we observed the fusion of pinpoint vesicle-like structures in close proximity to the plasma membrane (Fig. S5). This earliest ligand-induced fusion event was common to cells expressing wt Cbl, V431A, or F434A (Figs. S3-S5). In the absence of ultrastructural studies, it was not possible to establish in each transfected population whether the small structures were open plasma membrane invaginations or closed vesicles near the cell surface. Because the tiny structures in V431A-expressing cells were so dissimilar to the moderate-to-

large-sized vesicles scored in wt and F434A Cbl-expressing cells, no comparable fusion rate was determined for V431A.

The Cox proportional hazard regression analysis, using the robust sandwich method to account for the correlation of observed outcomes from the same image, was performed to test for the difference in the endosome fusion time distribution between GFP-Cbl wt and GFP-Cbl F434A. The Cox model included Plasmid Construct identity (GFP-Cbl wt vs. GFP-Cbl F434A), number of vesicles docked per cluster (2 vs. 3 or more), and the interaction of these factors, as independent variables. From the fitted Cox Model, there was a significant Construct*number docked interaction effect (p=0.001). Thus, the Construct effect on fusion time varied with the number of docked vesicles in a given cluster. The results for paired vesicles only are shown as Figure 4C. The median fusion time (25^{th}-75^{th} percentile) was 0.5 (range 0.5-1.0) minute for GFP-Cbl wt and 5.5 (range 1.5-14) minutes for GFP-Cbl F434A. Where the number of vesicles docked in a cluster was ≥3, construct effect was not significant (p=0.117). In this case, the median fusion time was 6 (range 1.5 to 15) minutes for GFP-Cbl wt and 11 (range 3 to >34) minutes for GFP-Cbl F434A. Based on these data and our previous report [9], we conclude that Cbl and its RF tail control EGF-R fate downstream in the endocytic pathway by enhancing the fusion of paired early endosomes, possibly via the regulation of phosphoHrs levels.

Discussion

We have investigated molecular events that regulate EGF-R fate and are modulated by the Cbl RF tail. Our results reveal that specific RF tail amino acids control EGF-R trafficking at biochemically distinct checkpoints. The first checkpoint is early in endocytosis, where Cbl regulates the ubiquitination and degradation of hSprouty2. The RF tail mutant V431A, compromised at this stage, fails to effect hSprouty2 degradation. Consistent with this result, in live cell imaging analysis, Cbl V431A induces the accumulation of small GFP/EGF-R-positive puncta that remain at the cell surface (Fig. S5).

The second checkpoint is at a later stage of endocytosis, where Cbl controls the apparent dephosphorylation and/or degradation of the trafficking regulator Hrs and also early endosome fusion (defective in mutant F434A). The identification here of a Cbl-regulated endosome fusion checkpoint is novel: it constitutes the first cell biological evidence that Cbl, as endocytic cargo, regulates EGF receptor fate by controlling the maturation of early endosomes.

The correlation between timely Hrs dephosphorylation/degradation and endosome fusion implies causation. However, definitive data from Hrs mutants that lack or mimic tyrosine phosphorylation at specific sites will be necessary to establish a causal link between the regulation of Hrs dephosphorylation/degradation and endosome fusion.

Because Cbl is an established signaling suppressor of numerous receptor and non-receptor tyrosine kinases, our finding has broad applicability to the field of tyrosine kinase signal regulation. Like ligand-stimulated EGF-R, activated c-Met, PDGF-R, IL-2-R and GM-CSF-R modulate the tyrosine phosphorylation of Hrs [24,25]. We predict that the lysosomal degradation of these proteins is similarly dependent upon Cbl-mediated Hrs degradation and the enhancement of early endosome fusion. Endosomal Hrs has been shown to inhibit the homotypic fusion of early endosomes in vitro [26] and to facilitate the recycling of some receptors [27,28]. Phosphorylation may serve as a critical timing switch for Hrs polyubiquitination [29] and degradation. This would facilitate the subsequent association of ubiquitinated EGF-R with ubiquitin-binding endosomal proteins that escort receptors further along the degradative pathway. The results presented here are consistent with a need for phosphoHrs degradation prior to endosome fusion and EGF-R trafficking to lysosomes: these processes are collectively compromised by the Cbl F434A mutant. Interestingly, Hrs itself

undergoes EGF-induced ubiquitination [29] that may be Cbl-mediated. Further studies at the molecular level will define how Cbl's RF tail residues mediate Hrs dephosphorylation and/or degradation and how this process affects signaling from a variety of activated tyrosine kinases.

Finally, our functional analysis of RF tail alanine substitution mutants warrants a fresh view of the reported Cbl crystal structure. The RF tail was relatively well ordered in the solved co-crystal of Cbl residues 47-447 with the E2 protein UbcH7 [11]. This was attributed, at least in part, to crystal packing. Based on the structural results, it was postulated that RF tail amino acids I429, V430, D432, and P433 might be determinants of Cbl function, as the residues mediate intramolecular interactions with the four-helix bundle of the TKB domain. No structural significance was proposed for RF tail residues V431 and F434. We were therefore surprised that substitution of the RF tail residues engaged in intramolecular crystal interactions had no apparent impact in our functional assays, whereas the V431A and F434A substitutions did. Further investigations of RF tail activity may clarify the functional relevance of the reported Cbl structure.

Materials and Methods

Plasmids

pAlterMAX-HA-Cbl, pAlterMAX-EGF-R, pcDNA3GFP-Cbl wt, and FLAG-hSprouty2 have been reported [2,4]. Single amino acid Cbl RF tail substitution mutants were generated using the pAlterMAX mutagenesis system (Promega) with template pAlterMAX-HA-Cbl. Mutant sequences were subcloned into the vector derived from *Eco*RI / *Xba*I-digestion of pcDNA3GFP-Cbl-N [2].

Antibodies

Anti-Syk [sc-1240; (4D10) murine IgG_{2a}], anti-EGF receptor [sc-120; (528) murine IgG_{2a}], and anti-Cbl [sc-170; (C-15) rabbit polyclonal] antibodies were obtained from Santa Cruz Biotechnology, Inc. Primary antibodies recognizing GFP [Ab290; rabbit polyclonal; Abcam Ltd.], ubiquitin [NCL-UBIQ; rabbit polyclonal; Novocastra Laboratories Ltd. from Vector Laboratories, Inc.], EGF receptor [#06-129; sheep polyclonal for immunoblotting; Upstate Biotechnology, Inc.], phosphotyrosine [#05-321; (4G10) murine IgG_{2b}; Upstate Biotechnology, Inc.], and the FLAG epitope tag [(M2) murine IgG_1; Sigma] were purchased. Anti-human leukocyte antigen class I antibody [(ATCC W6/32) murine IgG_{2a}] was prepared by the University of Iowa Hybridoma Facility. Secondary detection reagents included AffiniPure rabbit anti-mouse IgG_1 Fc_γ region-specific antibody [#315-035-046; Jackson ImmunoResearch Laboratories, Inc.], (R)-phycoerythrin-conjugated $F(ab')_2$ fragment of anti-mouse IgG (H+L) [#115-116-146; goat polyclonal; Jackson ImmunoResearch Laboratories, Inc.], peroxidase-conjugated Protein A [#55901; ICN Pharmaceuticals, Inc.], and peroxidase-conjugated anti-sheep IgG, H+L [#402100; rabbit polyclonal; Calbiochem-Novabiochem Corporation].

Cells

HEK 293 human embryonic kidney and COS-7 cells were used within 15 and 30 passages, respectively, of recovery from liquid nitrogen. Cultures were maintained in Dulbecco's modified Eagle's medium containing 10% fetal bovine serum (FBS), 0.1 mM non-essential amino acids, 1 mM sodium pyruvate, 100 units/ml penicillin-streptomycin and 20 mM HEPES at 37°C, 5% CO_2.

Transient Transfection, EGF Stimulation, and Cell Lysate Preparation

Transient transfection, EGF stimulation, and harvest of HEK 293 cells were performed as described [2]. DNA input amounts were as follows: for Fig. 1 and 2, HEK 293 cells were transfected with pAlterMAX-EGF-R (0.05 μg per 10 cm dish), an expression construct for FLAG-tagged hSprouty2 (1 μg per 10 cm dish) where indicated, and either GFP or the indicated GFP-Cbl expression constructs (4 μg per 10 cm dish). Transfection efficiencies for HEK 293 experiments ranged from 10-30%. EGF was used at 100 ng/ml (17 nM; Sigma) for cell stimulation. This ligand concentration is high but within the physiologically relevant range [30].

Immunoprecipitation and Immunoblotting

The immunoprecipitation procedures used for these studies have been reported [2,4]. Gel-resolved proteins were transferred to polyvinylidene difluoride (PVDF) membranes. For anti-ubiquitin immunoblotting, immunoprecipitate filters were autoclaved in water for 10 min prior to filter blocking and protein immunodetection. Filter incubations with primary antibodies, secondary reagents and detection solutions were performed as recommended by the suppliers. Image J and ScionImage software were used to quantify relative signals within experiments.

Downregulation Assays

EGF-R downregulation assays were performed as previously described [2]. Transfected cultures were harvested and processed at 4°C, either without or following cell stimulation with EGF for the times indicated. The cells were stained intact for selective identification of surface EGF-R.

Confocal Fluorescence Microscopy of Fixed Cells and Live Cell Imaging

For confocal microscopy, GFP- or GFP-Cbl-expressing COS-7 cells were serum-starved, stimulated for 25 minutes with Alexa Fluor 647-labeled EGF, paraformaldehyde-fixed, and immunostained for localization of EEA1 (Texas Red-conjugated anti-mouse secondary antibody). Images were collected on a Zeiss 510 confocal microscope using a PlanApo 63x oil immersion objective [numerical aperture (NA) 1.4]. Live imaging of transfected COS-7 cells in OptiMEM (Invitrogen) with 0.5% FBS and 5% CO_2 at 37°C was performed using an Olympus IX-81 microscope, a PlanApo 100x oil immersion objective (NA 1.4), and a Hamamatsu Orca ER camera. For Figs. S3 and S4, image collection began approximately 15 minutes after the addition of Lysotracker Red (Invitrogen) and unlabeled EGF. For Fig. S5, the red signal corresponded to Alexa Fluor 647-conjugated EGF. Red and green signals were acquired with SlideBook software at 30-second intervals over a 30- or 40-minute collection period. In SlideBook, all images were deconvolved using the no neighbors deconvolution algorithm. Supporting Online Material movies were generated from sequential image files using ImageJ. All presented still images were processed identically using Adobe Photoshop CS.

Supplementary Material

Refer to Web version on PubMed Central for supplementary material.

Acknowledgments

We thank S. Ramaswamy and Rosmarie Friemann for enlightening discussions of the reported Cbl crystal structure. Jussara Hagen, Tom Moninger, and Gene Hess provided expert technical advice and assistance. The Figure 4C statistical analysis was performed by M. Bridget Zimmerman of the Biostatistics Consulting Center, Department of Biostatistics, University of Iowa. Facilities at the University of Iowa College of Medicine (Flow Cytometry, Crystallography, DNA, Central Microscopy Research and Tissue Culture/Hybridoma facilities) were used for these studies.

This research was funded by: American Cancer Society Research Scholar Grant RSG-03-046-01 and NIH award RO1 CA109685 (to N.L.L.); an individual allocation from the American Cancer Society Institutional Research Grant IRG-122-V (from George Weiner at the Holden Comprehensive Cancer Center to N.L.L.); institutional training grants NRSA T32 DEO14678-03 and DEO14678-04 (from NIDCR to Christopher Squier and the Dows Institute and College of Dentistry at the University of Iowa, for support of N.L.L. and K.A.C., respectively); and grant BCTR0707177 from Susan G. Komen for the Cure (to J.G.K.).

References

1. Levkowitz G, Waterman H, Zamir E, Kam Z, Oved S, Langdon WY, Beguinot L, Geiger B, Yarden Y. c-Cbl/Sli-1 regulates endocytic sorting and ubiquitination of the epidermal growth factor receptor. Genes Dev 1998;12:3663–36674. [PubMed: 9851973]
2. Lill NL, Douillard P, Awwad RA, Ota S, Lupher ML Jr. Miyake S, Meissner-Lula N, Hsu VW, Band H. The evolutionarily conserved N-terminal region of Cbl is sufficient to enhance down-regulation of the epidermal growth factor receptor. J. Biol. Chem 2000;275:367–377. [PubMed: 10617627]
3. Duan L, Miura Y, Dimri M, Majumder B, Dodge IL, Reddi AL, Ghosh A, Fernandes N, Zhou P, Mullane-Robinson K, Rao N, Donoghue S, Rogers RA, Bowtell D, Naramura M, Gu H, Band V, Band H. Cbl-mediated ubiquitinylation is required for lysosomal sorting of epidermal growth factor receptor but is dispensable for endocytosis. J. Biol. Chem 2003;278:28950–28960. [PubMed: 12754251]
4. Visser GD, Lill NL. The Cbl RING finger C-terminal flank controls epidermal growth factor receptor fate downstream of receptor ubiquitination. Exp. Cell Res 2005;311:281–293. [PubMed: 16246327]
5. Haglund K, Sigismund S, Polo S, Szymkiewicz I, Di Fiore PP, Dikic I. Multiple monoubiquitination of RTKs is sufficient for their endocytosis and degradation. Nat. Cell Biol 2003;5:461–466. [PubMed: 12717448]
6. Mosesson Y, Shtiegman K, Katz M, Zwang Y, Vereb G, Szollosi J, Yarden Y. Endocytosis of receptor tyrosine kinases is driven by monoubiquitylation, not polyubiquitylation. J. Biol. Chem 2003;278:21323–21326. [PubMed: 12719435]
7. Huang F, Kirkpatrick D, Jiang X, Gygi S, Sorkin A. Differential regulation of EGF receptor internalization and degradation by multiubiquitination within the kinase domain. Mol. Cell 2006;21:737–748. [PubMed: 16543144]
8. Umebayashi K, Stenmark H, Yoshimori T. Ubc4/5 and c-Cbl continue to ubiquitinate EGF receptor after internalization to facilitate polyubiquitination and degradation. Mol. Biol. Cell 2008;19:3454–3462. [PubMed: 18508924]
9. Stern KA, Visser Smit GD, Place TL, Winistorfer S, Piper RC, Lill NL. Cbl enhances epidermal growth factor receptor degradation by modulating Hrs tyrosine phosphorylation. Mol. Cell. Biol 2007;27:888–898. [PubMed: 17101784]
10. Stern KA, Place TL, Lill NL. EGF and amphiregulin differentially regulate Cbl recruitment to endosomes and EGF receptor fate. Biochem. J 2008;410:585–594. [PubMed: 18045238]
11. Zheng N, Wang P, Jeffrey PD, Pavletich NP. Structure of a c-Cbl-UbcH7 complex: RING domain function in ubiquitin-protein ligases. Cell 2000;102:533–529. [PubMed: 10966114]
12. Wong ES, Lim J, Low BC, Chen Q, Guy GR. Evidence for direct interaction between Sprouty and Cbl. J. Biol. Chem 2001;276:5866–5875. [PubMed: 11053437]
13. Fong CW, Leong HF, Wong ES, Lim J, Yusoff P, Guy GR. Tyrosine phosphorylation of Sprouty2 enhances its interaction with c-Cbl and is crucial for its function. J. Biol. Chem 2003;278:33456–33464. [PubMed: 12815057]
14. Wong ES, Fong CW, Lim J, Yusoff P, Low BC, Langdon WY, Guy GR. Sprouty2 attenuates epidermal growth factor receptor ubiquitylation and endocytosis, and consequently enhances Ras/ERK signalling. EMBO J 2002;21:4796–4808. [PubMed: 12234920]
15. Hall AB, Jura N, DaSilva J, Jang YJ, Gong D, Bar-Sagi D. hSpry2 is targeted to the ubiquitin-dependent proteasome pathway by c-Cbl. Curr. Biol 2003;13:308–314. [PubMed: 12593796]
16. Mason JM, Morrison DJ, Bassit B, Dimri M, Band H, Licht JD, Gross I. Tyrosine phosphorylation of Sprouty proteins regulates their ability to inhibit growth factor signaling: a dual feedback loop. Mol. Biol. Cell 2004;15:2176–2188. [PubMed: 15004239]

17. Owen DJ, Vallis Y, Noble ME, Hunter JB, Dafforn TR, Evans PR, McMahon HT. A structural explanation for the binding of multiple ligands by the alpha-adaptin appendage domain. Cell 1999;97:805–815. [PubMed: 10380931]

18. Steen H, Kuster B, Fernandez M, Pandey A, Mann M. Tyrosine phosphorylation mapping of the epidermal growth factor receptor signaling pathway. J. Biol. Chem 2002;277:1031–1039. [PubMed: 11687594]

19. Urbe S, Sachse M, Row PE, Preisinger C, Barr FA, Strous G, Klumperman J, Clague MJ. The UIM domain of Hrs couples receptor sorting to vesicle formation. J. Cell Sci 2003;116:4169–4179. [PubMed: 12953068]

20. Bache KG, Raiborg C, Mehlum A, Madshus IH, Stenmark H. Phosphorylation of Hrs downstream of the epidermal growth factor receptor. Eur J Biochem 2002;269:3881–3887. [PubMed: 12180964]

21. Abella JV, Peschard P, Naujokas MA, Lin T, Saucier C, Urbe S, Park M. Met/Hepatocyte growth factor receptor ubiquitination suppresses transformation and is required for Hrs phosphorylation. Mol. Cell. Biol 2005;25:9632–9645. [PubMed: 16227611]

22. Row PE, Clague MJ, Urbe S. Growth factors induce differential phosphorylation profiles of the Hrs-STAM complex: a common node in signalling networks with signal-specific properties. Biochem. J 2005;389:629–636. [PubMed: 15828871]

23. Urbe S, Mills IG, Stenmark H, Kitamura N, Clague MJ. Endosomal localization and receptor dynamics determine tyrosine phosphorylation of hepatocyte growth factor-regulated tyrosine kinase substrate. Mol. Cell. Biol 2000;20:7685–7692. [PubMed: 11003664]

24. Asao H, Sasaki Y, Arita T, Tanaka N, Endo K, Kasai H, Takeshita T, Endo Y, Fujita T, Sugamura K. Hrs is associated with STAM, a signal-transducing adaptor molecule. Its suppressive effect on cytokine-induced cell growth. J. Biol. Chem 1997;272:32785–32791. [PubMed: 9407053]

25. Komada M, Kitamura N. Growth factor-induced tyrosine phosphorylation of Hrs, a novel 115-kilodalton protein with a structurally conserved putative zinc finger domain. Mol. Cell. Biol 1995;15:6213–6221. [PubMed: 7565774]

26. Sun W, Yan Q, Vida TA, Bean AJ. Hrs regulates early endosome fusion by inhibiting formation of an endosomal SNARE complex. J. Cell Biol 2003;162:125–137. [PubMed: 12847087]

27. Hanyaloglu AC, McCullagh E, von Zastrow M. Essential role of Hrs in a recycling mechanism mediating functional resensitization of cell signaling. EMBO J 2005;24:2265–2283. [PubMed: 15944737]

28. Yan Q, Sun W, Kujala P, Lotfi Y, Vida TA, Bean AJ. CART: an Hrs/actinin-4/BERP/myosin V protein complex required for efficient receptor recycling. Mol. Biol. Cell 2005;16:2470–2482. [PubMed: 15772161]

29. Polo S, Sigismund S, Faretta M, Guidi M, Capua MR, Bossi G, Chen H, De Camilli P, Di Fiore PP. A single motif responsible for ubiquitin recognition and monoubiquitination in endocytic proteins. Nature 2002;416:451–455. [PubMed: 11919637]

30. Sigismund S, Woelk T, Puri C, Maspero E, Tacchetti C, Transidico P, Di Fiore PP, Polo S. Clathrin-independent endocytosis of ubiquitinated cargos. Proc. Natl. Acad. Sci. U. S. A 2005;102:2760–2765. [PubMed: 15701692]

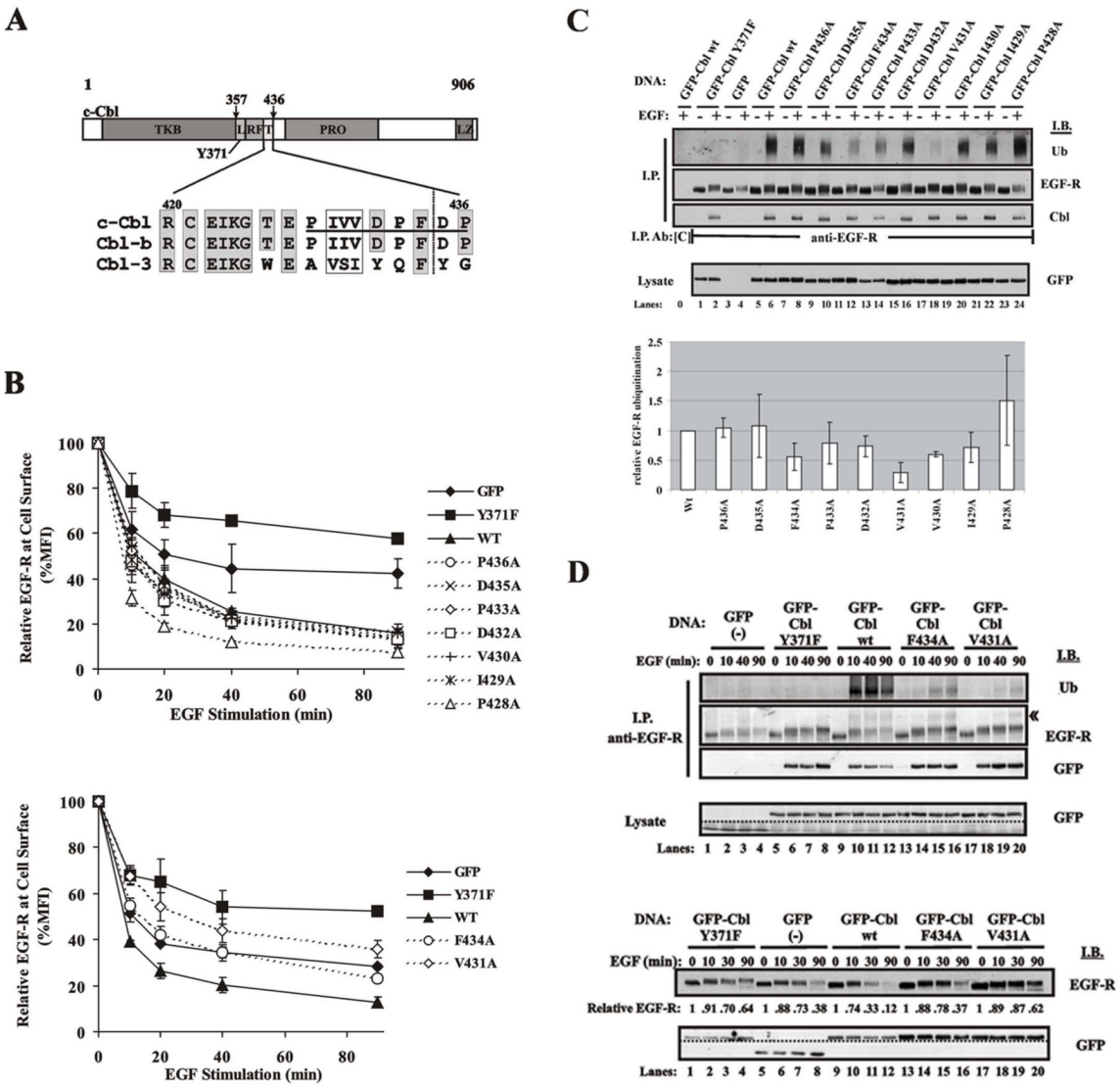

Figure 1. Biochemical characterization of Cbl RF tail alanine substitution mutants

A. The conserved C-terminal flank of the RING finger in human Cbl isoforms. Domains relevant to EGF-R regulation include: the tyrosine kinase-binding domain (TKB); linker region (L); RING finger domain (RF); RING finger C-terminal flank or "tail" domain (T); proline-rich region (PRO); and leucine zipper (LZ). Residue Y371 lies within the linker region. RING finger tail sequences of human Cbl isoforms (c-Cbl, Cbl-b, and Cbl-3) are aligned in the expanded portion of the graphic. Evolutionarily conserved sequences are marked with shaded (sequence identity) or plain (amino acid similarity) boxes. Underlined residues were substituted for this study. The vertical dashed line marks the C-terminal limit of the evolutionarily conserved Cbl sequences sufficient to enhance EGF-R ubiquitination, downregulation, and degradation. **B.** Cbl RF tail substitution mutants V431A and F434A are compromised for EGF-R downregulation. Surface EGF-R remaining at each stimulation time point was expressed relative to the amount of surface receptor in matched unstimulated cells. Results reflect the mean of three independent experiments ± S.D. **C.** Cbl RF tail substitution mutants V430A, V431A and F434A effect reduced EGF-R ubiquitination after 10 minutes of cell incubation with EGF. Upper section: 750 μg immunoprecipitates (anti-EGF-R antibody 528). Isotype-matched anti-Syk antibody 4D10 [C] was the specificity control. Immunoprecipitates (**I.P.**)

and 75 μg lysate protein samples were gel-resolved and sequentially immunoblotted (**I.B.**). Lower section: Quantification of results. Ub signals were normalized to their matching EGF-R signals. Mean values were expressed relative to the signal achieved with GFP-Cbl wild type (1.00). Results represent data from three independent experiments +/− S.D. Using Student's t-test with α=0.05, only V431A and V430A produced significantly less EGF-R ubiquitination than wt Cbl. **D.** Cbl mutants F434A and V431A effect reduced and delayed EGF-R ubiquitination and reduced EGF-R degradation. Upper section: 1 mg anti-EGF-R (528) immunoprecipitates. I.P.s (top three panels) and 100 μg of lysate protein from each sample (bottom panel) were sequentially immunoblotted using the antibodies indicated. The double claret marks the position of the predominant species of ubiquitinated EGF-R. Lower section: Quantification of EGF-R degradation effected by wild type and RF tail mutant Cbl proteins (100 μg protein/lane).

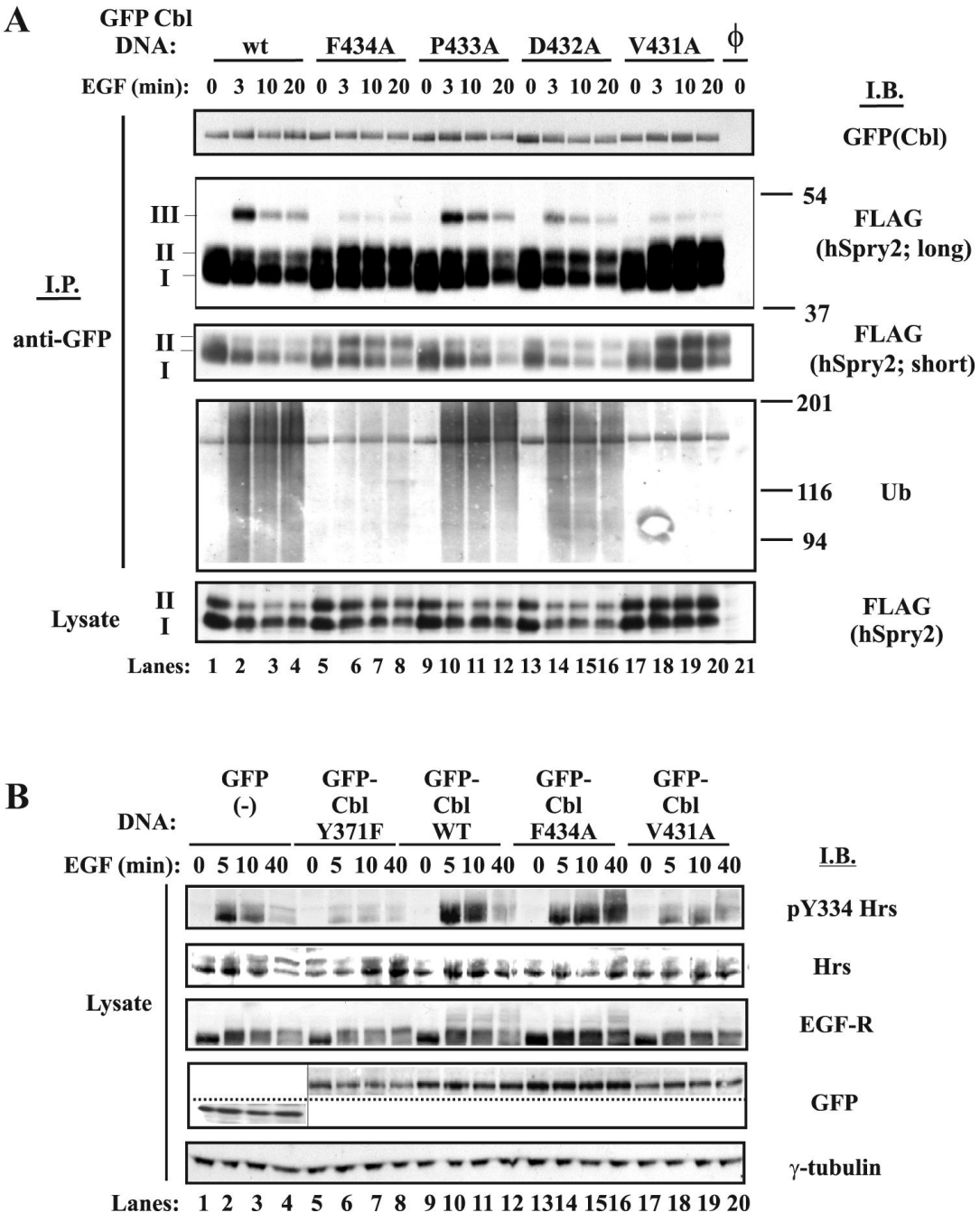

Figure 2. Aberrant regulation of hSprouty2 and Hrs by RF tail substitution mutants

A. Cbl mutants V431A and F434A are grossly and moderately compromised, respectively, for ubiquitin-associated degradation of the regulatory protein hSprouty2, but they are not defective in hSprouty2 binding. Immunoprecipitates (1 mg lysate protein per reaction; upper panels, **I.P.**) and 100 μg lysate samples (bottom panel) were gel-resolved and probed sequentially with the indicated antibodies (**I.B.**). I and II mark the more abundant species of hSprouty2. Both undergo rapid EGF-induced degradation in the presence of functionally wild type Cbl (bottom panel: wt, P433A and D432A). Species III may represent ligand-induced, ubiquitinated hSprouty2. The ligand-induced increase in Cbl/hSprouty2 complexes is best visualized in lanes 17-20, where expression of Cbl mutant V431A blocks the degradation of associated hSprouty2

(second panel). Equivalent masses of lysate protein contained comparable amounts of the GFP-Cbl proteins (top panel). **B.** Cbl RF tail mutant F434A effects Hrs tyrosine phosphorylation with kinetics like wild type Cbl, but the mutant is compromised for apparent Hrs dephosphorylation and/or degradation. For each sample, 100 μg of cell lysate protein was immunoblotted (**I.B.**) with the indicated antibodies. The γ-tubulin blot shows comparable protein loading in all lanes.

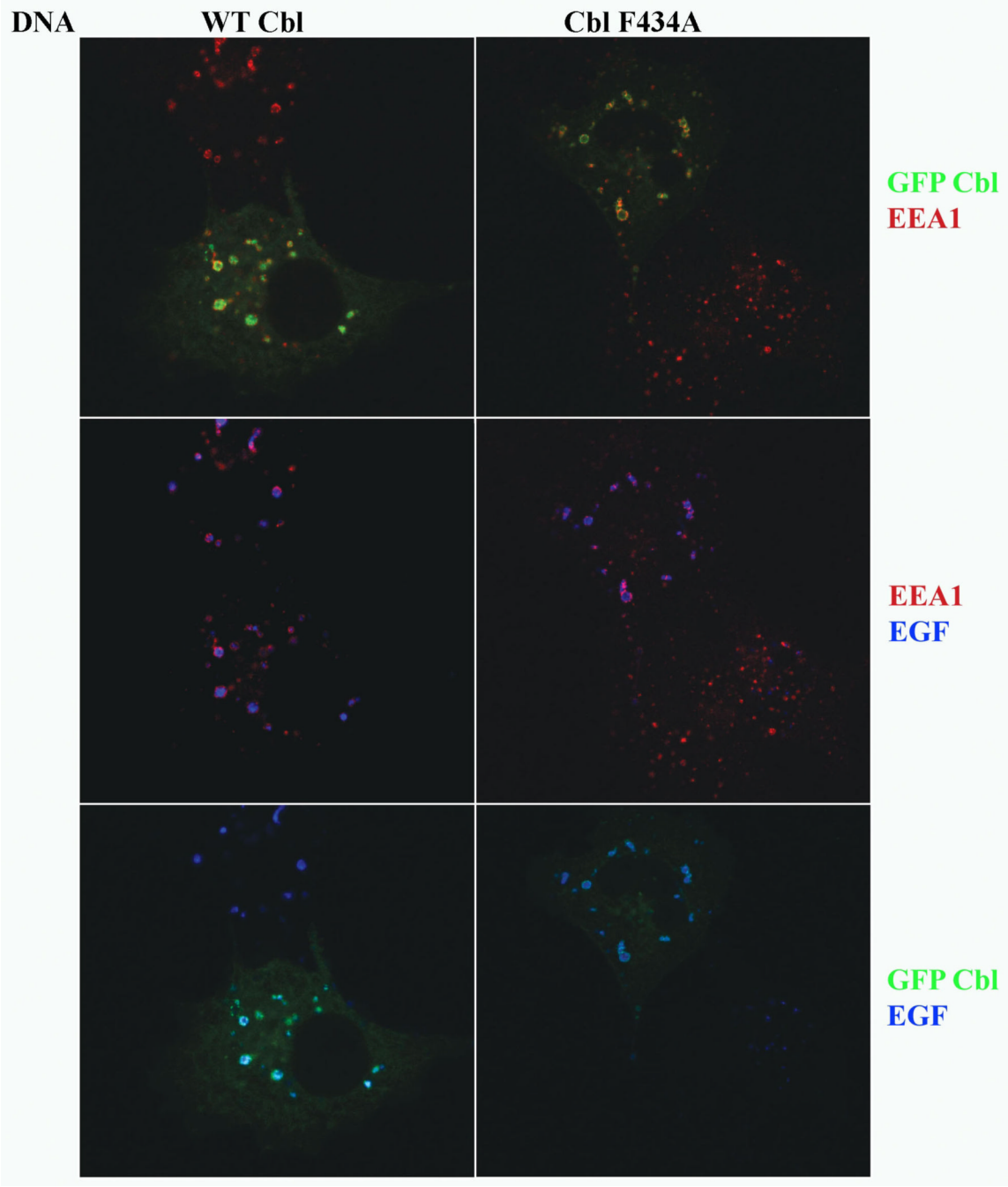

Figure 3. Cbl RF tail mutant F434A induces the aberrant pairing and clustering of early endosomes carrying activated EGF-R

COS-7 cells expressing endogenous EGF-R were transfected with the indicated GFP-Cbl expression constructs (4 μg per 10 cm dish). The cultures were stimulated with Alexa Fluor 647-EGF for 25 min, paraformaldehyde-fixed, and immunostained with anti-EEA1 antibody and a Texas Red secondary conjugate prior to visualization of the GFP-Cbl, EGF, and EEA1 signals. In five independent experiments, expression of the Cbl F434A mutant increased apparent endosome pairing and clustering. Localization of EEA1 to EGF- and GFP-Cbl-positive, clustered endosomes identifies the compartments as early endosomes. Protein colocalization within the figure is indicated by the following colors: top row, red plus green

yields yellow/orange; middle row, red plus blue yields magenta; bottom row, green plus blue yields aqua/light blue (compare with the darker blue signal of the upper cell in the bottom left panel). Several examples of vesicles exhibiting protein colocalization are marked by the white arrows.

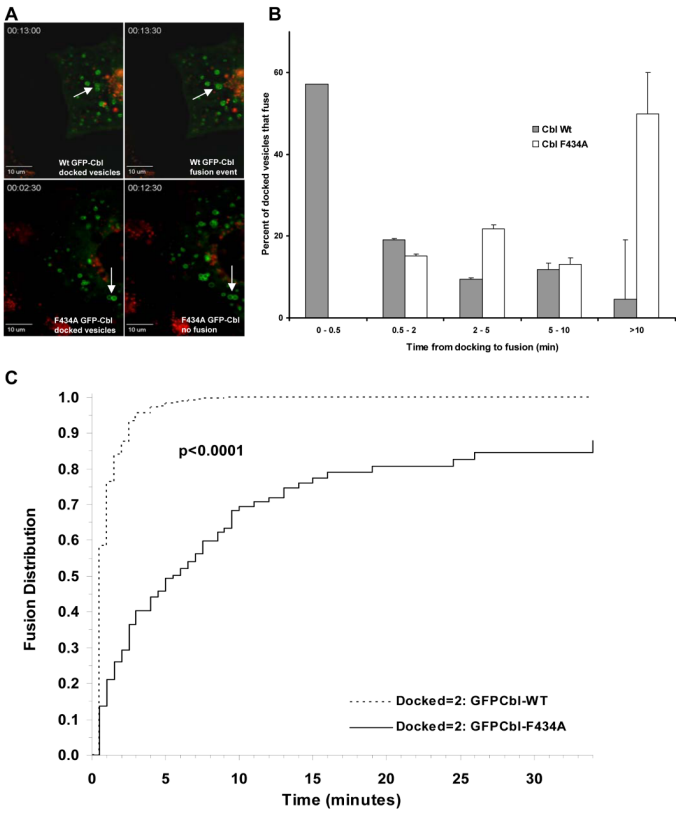

Figure 4. Deregulation of the Hrs checkpoint by Cbl mutant F434A impedes early endosome fusion

A. Select images from live cell collections (Figs. S3-S5) contrast the rapid fusion of endosomes bearing wild type GFP-Cbl with the delayed fusion of docked endosomes carrying GFP-Cbl F434A. Moderate-to-large endosomes rarely developed in Cbl V431A-expressing cells, which are shown here at reduced magnification to illustrate their distinct appearance. Note the difference in elapsed time for the paired images. For Cbl wt and F434A, Lysotracker Red-positive compartments are lysosomes. V431A images show red signal for fluor-conjugated EGF. Arrows mark the same paired vesicles at the early and later collection times. **B.** Fusion time was quantified from all docking events observed in movies for nine GFP-Cbl wt live cells and twelve GFP-Cbl F434A cells. Time to fusion (x-axis) is expressed relative to independent vesicle docking times, rather than from a single time point in the collection process. Standard deviations (error bars) were calculated from pooled experimental data. **C.** Cox proportional hazard regression analysis of fusion events for paired docked vesicles. Fusion occurred sooner in the GFP-Cbl wt-expressing cells compared to GFP-Cbl F434A expressors ($p<0.0001$). The graph shows the fusion distribution based on the fitted Cox model.